Available online at www.sciencedirect.com
SCIENCE DIRECT
Biochimica et Biophysica Acta 1757 (2006) 106–114
BIOCHIMICA ET BIOPHYSICA ACTA
BBA
http://www.elsevier.com/locate/bba

Herbicide binding and thermal stability of photosystem II isolated from *Thermosynechococcus elongatus*

K. Zimmermann [a,1], M. Heck [a,1], J. Frank [b,*], J. Kern [b], I. Vass [c], A. Zouni [b,*]

[a] *Institute for Medical Physics and Biophysics, Charité-Universitätsmedizin, D-10098 Berlin, Schumann Str. 21/22, Germany*
[b] *Max-Volmer-Laboratory for Biophysical Chemistry and Biochemistry, Institute for Chemistry, Technical University Berlin, D-10623 Berlin, Strasse des 17. Juni 135, Germany*
[c] *Institute of Plant Biology, Biological Research Center, H-6701 Szeged, P. O. Box 521, Hungary*

Received 10 August 2005; received in revised form 30 November 2005; accepted 5 December 2005
Available online 29 December 2005

Abstract

Binding of herbicides to photosystem II inhibits the electron transfer from Q_A to Q_B due to competition of herbicides with plastoquinone bound at the Q_B site. We investigated herbicide binding to monomeric and dimeric photosystem II core complexes (PSIIcc) isolated from *Thermosynechococcus elongatus* by a combination of different methods (isothermal titration and differential scanning calorimetry, CD spectroscopy and measurements of the oxygen evolution) yielding binding constants, enthalpies and stoichiometries for various herbicides as well as information regarding stabilization/destabilization of the complex. Herbicide binding to detergent-solubilized PSIIcc can be described by a model of single independent binding sites present on this important membrane protein. Interestingly, binding stoichiometries herbicide:PSIIcc are lower than 1:1 and vary depending on the herbicide under study. Strong binding herbicides such as terbutryn stabilize PSIIcc in thermal unfolding experiments and endothermically binding herbicides like ioxynil probably cause large structural changes accompanied with the binding process as shown by differential scanning calorimetry experiments of the unfolding reaction of PSIIcc monomer in the presence of ioxynil. In addition we studied the occupancy of the Q_B sites with plastoquinone (PQ9) by measuring flash induced fluorescence relaxation yielding a possible explanation for the deviations of herbicide binding from a 1:1 herbicide/binding site model.

Keywords: Photosystem II; Herbicide; Binding constant; Calorimetry; Flash induced fluorescence

1. Introduction

In plants, green algae, and cyanobacteria, oxygenic photosynthesis is catalyzed by two protein/pigment complexes, photosystems I and II (PSI, PSII). They are located in the thylakoid membrane and utilise light energy to oxidize water. This process is initiated by light captured by chlorophyll *a* (Chla) in antenna proteins and channeled to the primary electron donor P680 of PSII located near the lumenal side in the reaction center (RC). P680 is formed by a pair of Chla that are coordinated to the membrane embedded protein subunits D1 and D2 (for recent review on photosynthesis, see [1]). Initial charge separation occurs when light-activated P680* reduces a nearby pheophytin (pheo) to form the $P680^+pheo^-$ state. $Pheo^-$ reduces a bound plastoquinone (PQ9) known as Q_A while $P680^+$ oxidizes a redox-active

Abbreviations: Atrazin, 2-chloro-4-ethylamino-6-isopropylamino-1,3,5-triazin; Bromacil, 5-bromo-3-sec-butyl-6-methyluracil; Bromoxynil, 3,5-dibromo-4-hydroxybenzonitrile; Chla, chlorophyll a; 2,6-DBQ, 2,6-dichloro-p-benzoquinone; DCMU, 3-(3,4-dichlorophenyl)-1,1-dimethylurea; DLS, dynamic light scattering; β-DM, n-Dodecyl-β-D-maltoside; DSC, differential scanning calorimetry; Ioxynil, 3,5-diiodo-4-hydroxybenzonitrile; ITC, isothermal titration calorimetry; M, molecular mass; MES, 2-(N-morpholino)ethanesulfonic acid; PIPES, piperazine-*N*,*N*′-bis(2-ethanesulfonic acid); PQ9, plastoquinone 9; PSIIcc, photosystem II core complex; Terbutryn, 2-t-butylamino-4-ethylamino-6-methylmercapto-s-triazine; Trietazin, 2-chloro-4-diethylamino-6-ethylamino-s-triazin; TRIS, tris-(hydroxymethyl)-aminomethane

* Corresponding authors. Tel.: +49 30 314 25580; fax: +49 30 314 21122.
E-mail addresses: frank@phosis1.chem.tu-berlin.de (J. Frank), zouni@phosis1.chem.tu-berlin.de (A. Zouni).
[1] These authors contributed equally to this work.

0005-2728/$ - see front matter © 2005 Elsevier B.V. All rights reserved.
doi:10.1016/j.bbabio.2005.12.002

tyrosine (Y_z) to form the charge-separated state $Y_zQ_A^-$. A tetranuclear manganese (Mn) cluster near Y_z is oxidized by the tyrosine in a series of oxidation states (S-states), which are coupled to the oxidation of water to O_2 [2–7]. The electron remaining on Q_A is transferred to another plastoquinone (Q_B) that is loosely bound at the Q_B binding site, forming the plastosemiquinone, Q_B^-. After another successive electron transfer from Q_A associated with the uptake of 2 H^+, Q_BH_2 is exchanged for plastoquinone PQ9 from the membrane-embedded plastoquinone pool [8,9].

Electron transfer from Q_A to Q_B is inhibited by a wide variety of plastoquinone (PQ) analogues that compete with PQ at the Q_B site. The most frequently studied classes of inhibitors that are widely used as herbicides are urea and triazine derivatives such as DCMU and atrazine [10–14].

Thylakoid membrane fragments from the thermophilic cyanobacterium *Thermosynechococcus elongatus* were extracted with β-DM. The solubilized monomeric and dimeric PSII core complexes (PSIIcc) were separated chromatographically [16] and are both functionally active [17]. Recently, the molar mass of PSIIcc (the oligomerization state of PSII) was studied with several biophysical methods [16] yielding molar masses of 756 and 441 kDa for dimer and monomer, respectively. Monomer and dimer possess the same subunits (at least 16 membrane intrinsic and 3 extrinsic proteins) and the same cofactor composition.

Besides the two proteins D1 and D2 forming the reaction center (RC) [17,18], the core complex contains two antenna proteins known as CP47 and CP43 which contain about 30 Chla and 8–10 carotenoid molecules and cytochrome b559 formed by subunits α (5 kDa) and *β* (9 kDa). Cyanobacterial PSIIcc contains three membrane extrinsic proteins, the 33-kDa protein, a 12-kDa protein and cytochrome c550 with a molecular mass of 17 kDa. In addition to these 9 proteins, the PSIIcc contain at least 10 smaller subunits in the range ≤10 kDa [15] of mostly unknown function.

Monomeric PSIIcc could not yet be crystallized while crystals of dimeric PSIIcc diffract to a maximal resolution of 2.9 Å [19] and were used for X-ray crystallography to determine a structural model of PSII at resolutions of 3.8 to 3.2 Å [19,20]. Despite biochemical analysis revealing the presence of more than 2 PQ9 molecules per RC in monomeric and dimeric PSIIcc [15] no PQ9 could be localised in the QB site in the recent 3.2 Å resolution electron density obtained from dark adapted PSIIcc crystals [19,21]. In addition, quality of the electron density around the Q_B pocket was inferior to the Q_A pocket, indicating a higher disorder in this region. The present work was initiated to characterise in more detail the occupancy of the Q_B site in our PSIIcc preparation as well as to study herbicide binding to well-characterised samples of monomeric and dimeric PSIIcc. This could provide means for crystallization experiments of PSIIcc with herbicides. The co-crystallization of dimeric PSIIcc with herbicides might be useful to overcome micro-heterogeneity due to partial occupied Q_B sites and would allow to investigate the interaction of herbicides with functionally active PSII core complexes in molecular detail.

2. Materials and methods

All chemicals used in the present work were of analytical grade. Water was deionized through a Millipore-Q device. The following buffers were applied: Buffer A: 100 mM PIPES, pH 7.0, 0.03% β-DM and 5 mM $CaCl_2$. Buffer B: 20 mM MES-NaOH, pH 6.0, 0.02% β-DM, 20 mM $CaCl_2$, 25 mM $MgSO_4$, 5% glycerol. Buffer C: 20 mM MES-NaOH, pH 6.0, 20 mM $CaCl_2$, 10 mM $MgCl_2$. All three buffers support oxygen evolution with maximal rates between pH 6.0 and pH 7.0 and are optimal for all kind of studies as demonstrated in this publication. For the determination of the heat evolved due to proton release into the buffer accompanying the binding reaction between terbutryn and PSIIcc monomer, the following buffer solutions were used: Buffer D: 50 mM phosphate, pH 7.5, 5 mM $MgCl_2$, 0.02% β-DM. Buffer E: 50 mM PIPES, pH 7.5, 5 mM $CaCl_2$, 0.02% β-DM. Buffer F: 50 mM TRIS, pH 7.5, 5 mM $CaCl_2$, 0.02% β-DM.

2.1. Protein purification

Oxygen-evolving PSIIcc was extracted from thylakoid membranes of *T. elongatus* [22], purified and separated into two fractions by anion exchange chromatography, hereafter designated as fraction I and fraction II [15] that were subsequently identified as monomeric and dimeric PSIIcc, respectively [15,16].

2.2. Determination of protein and chlorophyll concentrations

Absorbance spectra were recorded at room temperature using a Shimadzu UV 3000 spectrophotometer with an optical pathlength of 1 cm. Chla concentrations were determined after extraction with 80% acetone [23]. The protein concentrations of PSIIcc were calculated by assuming that 35 Chla are bound per P680, respectively [19,24,25].

2.3. Herbicide binding to PSIIcc detected by isothermal titration calorimetry

Isothermal titration calorimetry (ITC) experiments of herbicide binding to monomeric and dimeric PSIIcc were performed in buffer A at 25 °C using the MCS-calorimeter manufactured by MicroCal, Inc. (Northampton, MA). For description, design and operation of this instrument see [26,27]. For measurements of the heat production accompanying the binding of different herbicides to PSIIcc, the protein was loaded into the sample cell of the calorimeter (volume ≈ 1.4 ml), and the reference cell was filled with distilled water. A 100-mM stock solution of different herbicides dissolved in DMSO was diluted with buffer A to 0.5 or 1 mM. Buffer solutions were degassed by stirring under vacuum before use. Samples were prepared under ambient light. Solutions of 0.5 or 1 mM herbicide were then filled either into 100 µl or 250 µl syringes. The final yield of DMSO was adjusted to 1% v/v in calorimeter cell and syringe. The system was allowed to equilibrate until a stable baseline was observed before an automated titration was initiated. A typical experiment involved 30 injections of 8 µl of the herbicide solutions into the sample cell containing 25–30 µM monomeric or dimeric PSIIcc reaction centers in ≈1.4 ml buffer A at time intervals of 5 min. Throughout the titration the cell was stirred continuously at 400 rev./min. The data obtained were evaluated to determine the binding stoichiometry n for PSIIcc monomer or dimer, the binding constant K and the enthalpy change ΔH_b by non-linear least square analysis for a single set of identical binding sites [27]. The statistical error for the stoichiometry, n, obtained from the fitting routine is typically 2–3%. This value is too low and should be 5% due to pippeting the solutions with an additional error of 5% for the whole ITC procedure. Therefore, we use in this publication an error for the stoichiometry, n, of 10%. To obtain the fit parameters n, K and ΔH_b we used single experiments or experiments in duplicate with similar results.

2.4. ITC data evaluation

The area of the first injection tend to be smaller than it should be. We followed the recommendation of Microcal and set the volume of the first

injection to 3 μl; the corresponding point was removed before curve-fitting was carried out on the integrated data.

Heat changes registered after full saturation are caused by the heat of ligand dilution. The heat of the last injections after completion of the binding curve were averaged and subtracted as reference.

2.5. Herbicide binding and thermal stability of monomeric and dimeric PSIIcc measured by DSC

Differential scanning calorimetry (DSC) experiments of PSIIcc were performed in the presence of 0.5 mM herbicide in a MicroCal Capillary DSC with Autosampler (MicroCal, Northampton, MA) at a PSIIcc protein concentration of 0.4 mg/ml (0.91 μM monomer and 0.56 μM dimer) in buffer A at pH 7.6 between 20 and 100 °C at a scan rate of 60 °C per hour. Samples were prepared under ambient light. The pressure was maintained above 1.5 bar to prevent degassing of the samples at higher temperatures. Heat capacity C_p (J/°C) was measured as a function of temperature (°C). C_p was converted to the molar heat capacity C_p^m (kJ mol^{-1} °C^{-1}) accounting for volume (V=130 μl) and sample concentration. Phase transition temperatures T_m (°C) of PSIIcc were obtained at the highest molar heat capacity C_p^m from the DSC curves after subtraction of both the re-scan (after thermal unfolding) and the baseline.

The area under the DSC curve corresponds to the molar enthalpy change ΔH_{cal} (kJ/mol) for the phase transition. Data analysis for all experiments was performed by using MicroCal Origin software.

2.6. Inhibition of oxygen evolution by herbicides

Oxygen evolution measurements were conducted at RT using a home built Clark type electrode [28]. PSIIcc was excitated with saturating continuous white light from a tungsten lamp passed through a heat filter. Monomeric PSIIcc samples were diluted to 20–50 μM Chla with buffer C that was used for all oxygen evolution measurements. As artificial electron acceptor 2 mM 2,6-dichloro-p-benzoquinone (2,6-DBQ) was added. The electrode was calibrated using air-saturated and nitrogen-saturated water at atmospheric pressure. In the presence of herbicides (between 1×10^{-10} M and 1×10^{-3} M) the rate of the oxygen evolution decreases yielding stable rates which were lower compared with the rate at zero herbicide concentration.

$$I(\text{normalized}) = \frac{\text{rate(herbicide} = 0) - \text{rate(with herbicide)}}{\text{rate(herbicide} = 0)}, \quad 0 \le I(\text{normalized}) \le 1 \tag{1}$$

half-logarithmic plots of the normalized inhibition as function of the herbicide concentration yielded s-shaped curves typical for binding data with an apparent $K_{i,app.}$ for half-maximal inhibition and I_{max} for maximal inhibition. $K_{i,app.}$ values are comparable with K_d values derived from ITC-experiments if one assume competitive inhibition for the binding of herbicides to monomeric and dimeric PSIIcc. The artificial electron acceptor 2,6-DBQ does not interfere with herbicide binding as demonstrated for terbutryn by ITC experiments (data not shown).

2.7. Flash-induced fluorescence relaxation kinetics

Flash-induced increase and the subsequent decay of chlorophyll fluorescence yield were measured by a double-modulation fluorometer (PSI Instruments, Brno) [29] in the 150 μs to 100 s time range as described earlier [30]. The sample concentration was 5 μg ml^{-1} Chla. Multicomponent deconvolution of the measured curves was done by using a fitting function with two exponential and one hyperbolic components:

$$F(t) - F_0 = A_1\exp(-t/T_1) + A_2\exp(-t/T_2) + A_3/(1 + t/T_3) \tag{2}$$

where $F(t)$ is the variable fluorescence yield, F_0 is the basic fluorescence level before the flash, A_1–A_3 are the amplitudes, T_1–T_3 are the time constants. The non-linear correlation between fluorescence yield and the redox state of Q_A was corrected for using the Joliot model [31] with a value of 0.5 for the energy-transfer parameter between PSIIcc units.

2.8. Circular dichroism spectroscopy experiments

To compare the phase transition temperature T_m of the unfolding reaction measured by DSC we performed CD-spectroscopy with a Jasco J-500 spectropolarimeter. Response time, sensitivity and scan speed were 0.5 s, 50 mdeg. per full scale and 20 nm/min, respectively. Two scans were averaged in the far-UV region from 200 to 260 nm. The band width was 1.0 nm, resolution 0.1 nm. Monomeric and dimeric PSIIcc isolated and purified from *T. elongatus* was dissolved in buffer B, adjusted to 50 μg/ml protein concentration and transferred to a 2-mm wide quartz cuvette. To solutions of 66 nM dimeric PSIIcc (protein concentration), 1 μM ioxynil, 1 μM DCMU or 1 μM atrazin each were added and measured as described above. The denaturation curve was analyzed with the nonlinear Boltzmann equation of the Origin 6.0 program (OriginLab Corporation, Northampton, MA) to derive the melting temperature T_m [32]. By assuming a two-state reversible equilibrium process between the native (F) and denaturated states (U) the fraction of denaturated protein, f_u, at temperature, T, was determined according to Eq. (3):

$$f_U = \frac{\Theta_{T,220} - \Theta_F}{\Theta_U - \Theta_F} \tag{3}$$

where $\Theta_{T,220}$ is the measured ellipticities at 220 nm and temperature T. Θ_F and Θ_U are the ellipticity at 220 nm of totally folded and unfolded states measured at 25 °C and 95 °C, respectively.

3. Results

3.1. Content of PQ9 in Q_B sites

The amount of PQ9 bound to the Q_B site as well as its replacement by DCMU was studied by flash-induced chlorophyll fluorescence measurements. Illumination of monomeric or dimeric PSIIcc with a single turnover saturating flash induces reduction of Q_A, which leads to increased fluorescence yield. Subsequent reoxidation of Q_A^- in the dark results in relaxation of fluorescence yield that exhibits three main decay phases. The origin of the decay phases can be assigned to forward and backward electron transport reactions (see refs. [9,33,34]) as summarized below. The fast phase, which contributes to ~52% of the total relative decay amplitude with T_1 ~780 μs time constant in dimeric PSIIcc (Fig. 1 and Table 1), arises from the reoxidation of Q_A^- by PQ9 molecules bound to the Q_B site before the flash. The middle phase, T_2 ~9 ms time constant and A_2 ~24% relative amplitude, originates from Q_A^- reoxidation by PQ9 molecules in centers where the Q_B site was empty at the time of the flash. Finally the slow phase, T_3 ~5 s time constant and A_3 ~24% relative amplitude, arises from back reaction of Q_A^- with the S_2 state of the water-oxidizing complex.

In monomeric PSIIcc, the fast and middle phases are slower (T_1 ~3.7 ms and T_2 ~35 ms, respectively) and smaller (30 and 11%, respectively) than in the dimers, whereas the amplitude of the slow phase is substantially increased (~60%). When the Q_A to Q_B electron transfer step is blocked by DCMU, the reoxidation of Q_A^- proceeds via charge recombination with donor side components. The main phase of the decay arises from the recombination of Q_A^- with the S_2 state of the water oxidizing complex. The time constant of this phase is about 7 s in the dimers and 9 s in the monomers with 90 and 89% relative amplitudes, respectively. The fast phase of the decay in the presence of DCMU arises from the recombination of Q_A^- with

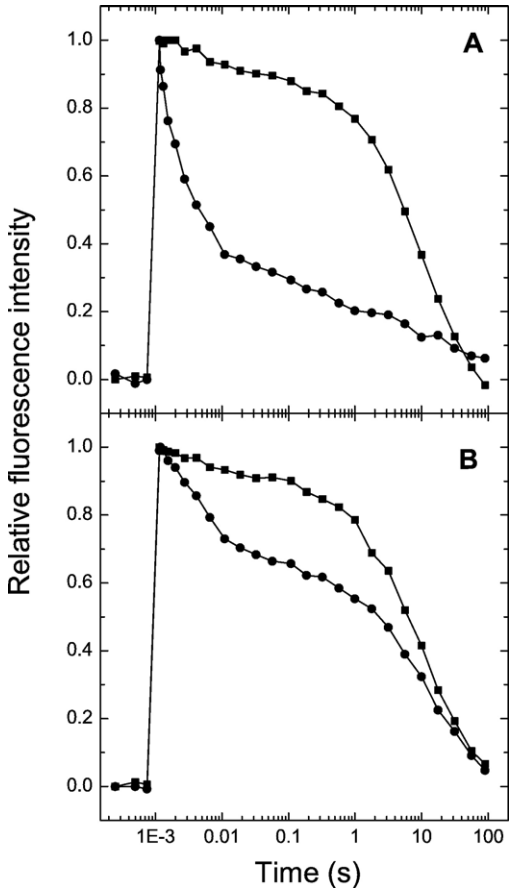

Fig. 1. (A, B) Relaxation of flash-induced chlorophyll fluorescence in PSIIcc particles. Dimeric (A) and monomeric (B) PSIIcc particles were excited by a single turnover flash fired at the 1-ms time point, and chlorophyll fluorescence relaxation was measured in the absence mm (circles) and presence (squares) of 10 μM DCMU. The curves are shown after normalization to the same initial amplitude.

Tyr-$Z^{\bullet}$ in centers in which the Mn cluster is not functional. The amplitude of this phase is only 10% showing that the majority of the cores retain fully functional water oxidizing complex. The significantly slowed fluorescence change in the presence of DCMU as compared to that in the absence of DCMU indicates that the Q_A to Q_B transfer is probably fully blocked in the absence of artificial acceptors.

Table 1
Kinetic parameters of flash-induced chlorophyll fluorescence decay in dimeric and monomeric PSIIcc particles

	Fast phase		Middle phase		Slow phase	
	τ (ms)	Amp (%)	τ (ms)	Amp (%)	τ/Amp (s)	Amp (%)
No addition						
Dimer	0.78±0.4	52±4	9±3	24±2	5.1±2.5	24±2
Monomer	3.7±0.5	30±7	37±15	11±2	9.9±0.7	59±5
DCMU						
Dimer	4.2±0.6	10±1			6.8±1.2	90±2
Monomer	12.1±1.5	11±1			9.1±1.8	89±2

Fluorescence traces were measured as in Fig. 1, and analyzed as described in Materials and methods.

3.2. Herbicide binding to PSIIcc as measured by ITC

To study the binding of herbicides to the partially blocked Q_B sites we applied isothermal titration calorimetry (ITC) and measured the inhibition of the oxygen-evolution by herbicides. The former experiment yielded besides stoichiometry, n, and dissociation constant, K_d, the enthalpy change, ΔH_b, associated with the binding reaction as displayed in Table 2a, b. Fig. 2 shows a typical result of an ITC experiment for the binding of terbutryn to monomeric PSIIcc. The dissociation constants, K_d, of all investigated herbicide/PSIIcc monomer complexes are found in the low micromolar range. Even the strongest binding herbicides like terbutryn or atrazin do not exhibit 1:1 stoichiometries, n, for herbicide:PSIIcc monomer complex formation. Stoichiometries vary over a wide range between $n=0.84$ for terbutryn and $n=0.202$ for bromacil resulting in the ranking of herbicides as shown in Table 2a.

All classes of herbicides except the benzonitrile type ioxynil and bromoxynil showed exothermic ITC curves. For ioxynil and bromoxynil, the enthalpy change ΔH_b associated with the binding reaction was positive (Fig. 3 and Table 2a, b).

To study proton uptake/release accompanying the binding reaction between terbutryn and monomeric PSIIcc the apparent values of ΔH_b for terbutryn were measured in three different buffers (D–F) of increasing heats of ionization. Plotting of the negative apparent enthalpy change due to the binding reaction as a function of the positive ionization enthalpy of the buffer solutions yielded a straight line with an intercept of $\Delta H'_b = -33.5\pm0.4$ kJ/mol and a slope of 0.41 ± 0.02 equivalent to the corrected binding enthalpy $\Delta H'_b$ without any neutralization reaction and a proton release to the buffer of 0.4 mol H^+ per mol terbutryn bound (data not shown).

Table 2
Binding parameters of herbicides to PSIIcc as measured by ITC

Herbicide	ΔH_b (kJ/mol)	n (n per monomer)	K_d (μM)
(a) PSIIcc monomer			
Terbutryn	−39.7±1*	0.84±0.08#	0.495±0.12*
Atrazin	−13.9±0.5*	0.61±0.06#	0.64±0.17*
DCMU	−9.9±0.75*	0.33±0.03#	0.76±0.29*
Bromacil	−44±12*	0.202±0.02#	0.96±0.37*
Trietazin	–	$n<0.1$	–
Ioxynil	+8.5±0.25*	0.82±0.08#	2.09±0.28*
Bromoxynil	+5.8±1*	0.29±0.03#	0.7±0.5*
(b) PSIIcc dimer			
Herbicide	ΔH_b (kJ/mol)	n (n per dimer)	K_d (μM)
Terbutryn	−32.8±13.8+	0.82±0.12+	0.54±0.34+
Ioxynil	+4.5±1*	2.2±0.2#	2.37±1.54*

Standard error of the mean (SEM) were obtained from a fit of the data points of the ITC-experiments and marked with (*). For terbutryn and dimeric PSIIcc, three independent experiments are performed. The standard deviation (SD) of these three experiments is given in (b) (+).
(a) Molar enthalpy change upon binding, ΔH_b, per mol herbicide, number of binding sites n, and dissociation constants K_d for the binding reaction between herbicides and monomeric PSIIcc as measured by isothermal differential titration calorimetry (ITC) applying PIPES buffer A at pH 7.0. (b) Binding reaction between herbicides and dimeric PSIIcc. The errors for the stoichiometries, n, were estimated to be 10% (#).

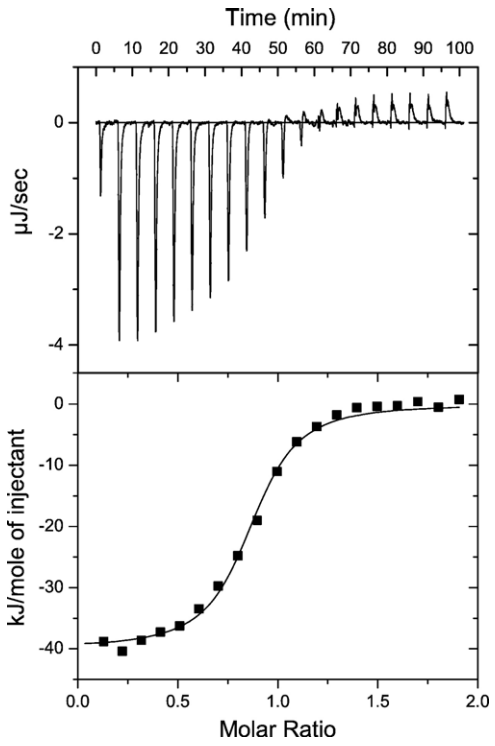

Fig. 2. (a, b) Diagram of the heat per injectant (lower part) and of the enthalpy produced in each of 20 injections of 8 µl of 0.5 mM terbutryn into a solution of 31.4 µM (12 mg/ml) monomeric PSIIcc in buffer A at 25 °C (upper part) measured by isothermal titration calorimetry (ITC). n and K_d are determined to be 0.84±0.015 and 0.495±0.12 µM, respectively, for this data set. ΔH_b= −39.7±1 kJ/mol.

Binding of terbutryn to dimeric PSIIcc exhibits comparable dissociation constants K_d as observed for monomeric PSIIcc but of significant lower stoichiometries. Approximately only 50% of the binding sites of the dimer are saturable by terbutryn (Tables 2a, b, 3). In addition we tried to perform ITC experiments with thylakoid membrane fragments in spite of the low PSII content. Due to the low PSII content of thylakoids (approximately only 10% of the Chla content of thylakoids belong to PSII (data not shown)) very high concentrations of thylakoids (≥2.5 mM Chla) were necessary to increase the signals compared with the noise of the baseline. The baseline noise is strongly increased with high thylakoid concentrations because stirring of the thylakoid suspension produces heat. The titration of thylakoid membrane fragments isolated from *T. elongatus* at a concentration of 2.7 mM Chla in ≈1.4 ml by 30 injections of 8 µl of a 0.1-mM herbicide solution yielded signals close to the resolution (≥4.18 µJ per peak area) of the ITC apparatus and provided binding parameters n=0.24, K_d=1.3 µM and ΔH_b=−28.6 kJ/mol for terbutryn.

3.3. Inhibition of the steady-state oxygen-evolution of PSIIcc by herbicides

Virtually, the same ranking of herbicide binding to PSIIcc as measured with ITC was observed by competitive inhibition of the steady-state oxygen evolution due to herbicide binding to PSIIcc (Table 3 and Fig. 4). For analyzing the water splitting activities and the influence of herbicides on monomeric and dimeric PSIIcc, the oxygen evolution under continuous light was measured. Typical values obtained in the absence and presence of herbicides are shown in Table 3. Apparent inhibition constants, $K_{i,app.}$, (concentration of herbicide necessary for half maximal inhibition) and herbicide concentration, c, for maximal resistance against inhibition of oxygen evolution for different herbicides are displayed in Table 3. In the presence of 0.085 mM 2,6-DBQ as external electron acceptor, no change of the binding parameters for terbutryn is observed in ITC experiments. 2,6-DBQ binds only weakly to monomeric PSIIcc with a large amount of heat of dilution and/or the reaction enthalpy due to reduction of this artificial electron acceptor by PSIIcc in red light which illuminates the ITC cell (data not shown). This indicates that the artificial electron acceptor 2,6-dichloro-p-benzoquinone (2,6-DBQ) does not compete with herbicides bound in the Q_B site.

3.4. Thermal stability of PSIIcc measured by DSC experiments and CD spectroscopy

The stability of the monomeric and dimeric PSIIcc was also studied by CD-spectroscopy as function of temperature. The CD-spectra did not significantly change in the temperature range of 20 to 50 °C, however, above 60 °C dramatic spectral changes were observed. From the change of ellipticity at 220 nm the phase transition temperature for monomeric and dimeric PSIIcc

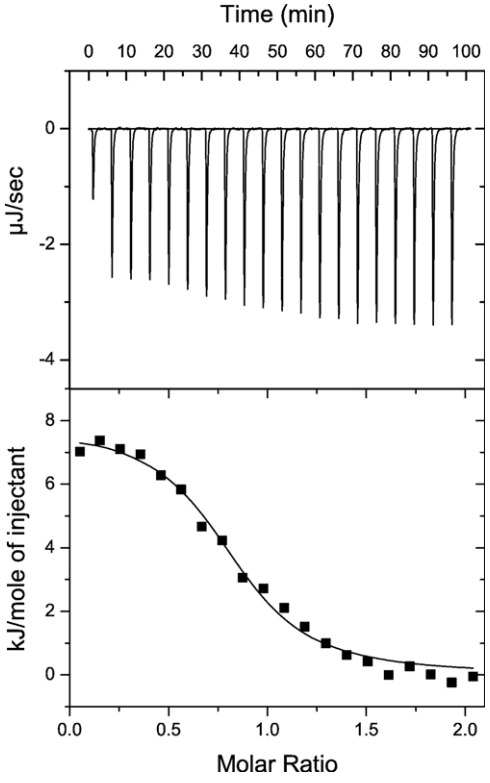

Fig. 3. (a, b) Diagram of the heat per injectant (lower part) and of the enthalpy produced in each of 20 injections of 8 µl of 1 mM ioxynil into a solution of 28.8 µM (11.3 mg/ml) monomeric PSIIcc in buffer A at 25 °C (upper part) measured by isothermal titration calorimetry (ITC). n and K_d are determined to be 0.82±0.02 and 2.09±0.28 µM, respectively, for this data set. ΔH_b= +8.5±0.25 kJ/mol.

Table 3
Inhibition of the oxygen evolution due to herbicide binding to PSIIcc

PSIIcc from *T. elongatus*	Continuous saturating light µmol O_2 (mg Chla·h)$^{-1}$
(a)	
Crude extract	200–450
Monomeric PSIIcc	1700–3000
Dimeric PSIIcc	2200–3700
Redissolved PSIIcc crystals	2000–2600
Herbicide (1×10^{-3} M)	**Continuous saturating light µmol O_2 (mg Chla·h)$^{-1}$**
(b)	
Terbutryn	240±50
DCMU	590±120
Bromoxynil	660±130
Ioxynil	240±50

Herbicide	I_{max} (%)	$K_{i,app.}$ (µM)
(c)		
Terbutryn	86.4±4	0.47±0.19
Atrazin	77.9±5.2	1.67±0.7
DCMU	70±4.6	0.76±0.23
Bromacil	71.3±1.2	1.32±0.22
Ioxynil	88.9±2.3	1.6±0.2
Bromoxynil	60.1±11.8	3.5±2.4
Terbutryn *	45.1±2	0.17±0.03

(a) Oxygen evolution activities for different PSII samples. Values are ranges obtained from at least 6 independent measurements for each sample type. (b) Residual oxygen evolving activity caused by 1 mM of several herbicides for monomeric PSIIcc. (c) Resistance against inhibition, herbicide concentration c ($K_{i,app}$) for half-maximal inhibition of oxygen evolution of monomeric PSIIcc by herbicides as indicated.
* Binding of terbutryn to PSIIcc dimer.

was determined to be 68 and 71 °C, respectively. Thermal unfolding of monomeric PSIIcc was unaffected by herbicides as measured by DSC and showed no shift to higher

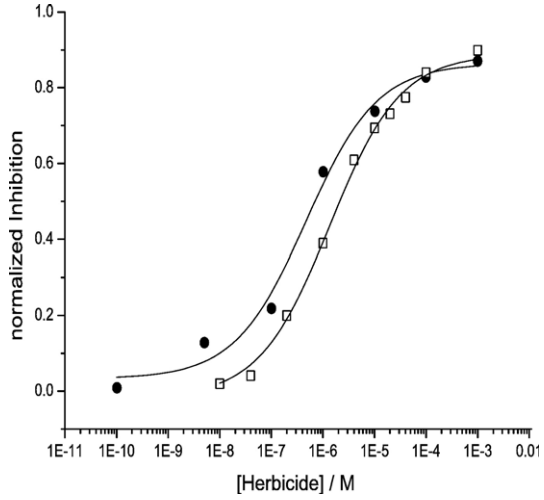

Fig. 4. Inhibition of oxygen-evolution activity by herbicide binding to monomeric PSIIcc. Binding of terbutryn (●) and ioxynil (□). I_{max} and $K_{i,app.}$ are determined to be 86.4±4% and 0.47±0.19 µM for binding of terbutryn to monomeric PSIIcc. For ioxynil I_{max} and K_i are determined to be 88.9±2.3% and 1.6±0.2 µM, respectively.

Table 4
ΔH_{cal} and T_m for the thermal unfolding reaction as measured by DSC experiments of monomeric and dimeric PSIIcc in the presence and absence of 0.5 mM herbicide as indicated

Herbicide	Monomeric PSIIcc ΔH_{cal} ($\times10^6$ kJ/mol)	T_m (°C)	Dimeric PSIIcc ΔH_{cal} ($\times10^6$ kJ/mol)	T_m (°C)
Without	7.46	72.2	11.1	70.0
Terbutryn	12.4	71.1	10.6	70.0
Atrazin	7.27	71.9	6.8	72.3
DCMU	9.32	70.9	10.3	71.8
Bromacil	7.73	71.3	9.8	71.0
Trietazin	9.82	71.2	2.4	70.8
Ioxynil	3.85	70.5	10	70.4
Bromoxynil	5.4	71.5	10.2	70.7

The phase transition curves for the thermal unfolding of dimeric PSIIcc show (beside the maximum at T_m) two shoulders around 60 and 77 °C (Fig. 5b). Experimental error: ΔH_{cal}=± 15%, T_m=±0.5 °C.

temperatures with increasing herbicides concentrations. The main phase transition T_m occurred at 71.1 °C in presence of all herbicide studied. In contrast to T_m, the enthalpy change ΔH_{cal} associated with the unfolding reaction as measured in DSC experiments is influenced by the herbicides studied (Table 4 and Fig. 5a, b). Terbutryn showed higher enthalpy change values than obtained for all other herbicides inclusive monomeric PSIIcc in the absence of herbicides. Ioxynil destabilizes monomeric PSIIcc by strongly decreasing the ΔH_{cal} value for the unfolding reaction.

The influence of herbicides on the thermal stability of dimeric PSIIcc is displayed in Table 4. Herbicides increase slightly T_m of dimeric PSIIcc by a maximum of about 2.3 °C measured for atrazin. This trend is also seen by CD spectroscopy for other herbicides measured at temperatures between 20 and 95 °C showing a maximal increase in T_m for atrazin (Table 5, Fig. 6).

4. Discussion

There are a number of studies in the literature concerning herbicide binding to PSII in thylakoid membrane fragments [35], but only few such investigations were performed with fully active detergent-solubilized PSIIcc [36] and none with the ITC-technique. Chromatographic analysis shows that more than one PQ9 (about 2.9±0.8) is present per PSIIcc [15], as reported for other PSIIcc preparations [37,38]. However in the electron density calculated from the X-ray diffraction of our crystals at 3.8 Å and at 3.2 Å resolution, respectively, no PQ9 could be detected in the Q_B pocket [19,39]. At 3.0 Å resolution, PQ9 could be located in the Q_B site in the electron density map but only at an occupancy of 50% (J. Biesiadka, personal communication).

Flash-induced chlorophyll fluorescence measurements performed on solutions of monomeric and dimeric PSIIcc, reveal that only 30% of monomeric and 50% of dimeric PSIIcc have a functional PQ9 bound to the Q_B site in dark adapted samples. An additional 24% of the dimeric and 11% of the monomeric PSIIcc can bind PQ9 at the Q_B site after illumination suggesting that the Q_B site is not fully occupied in our PSIIcc preparation.

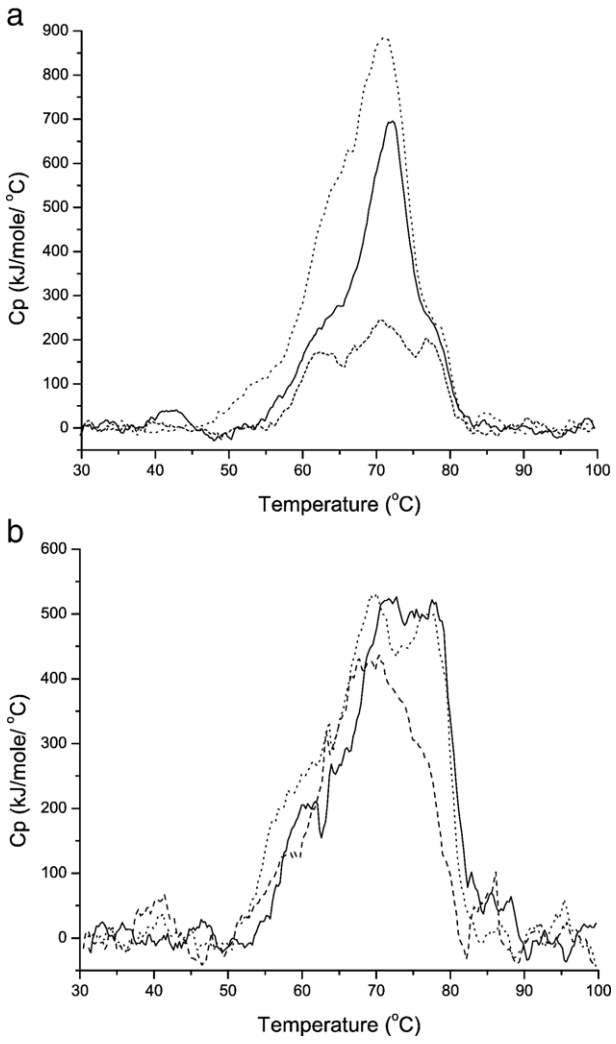

Fig. 5. (a, b) Differential scanning calorimetry (DSC) thermograms (after baseline correction) for the thermal denaturation of (a) monomeric (0.905 μM) and (b) dimeric (0.56 μM) PSIIcc containing either 0.5 mM terbutryn, 0.5 mM ioxynil or with no addition (Terbutryn, ···, dotted line); (*Ioxynil*, ---, dashed line); (without herbicides, —, solid line). The phase transition temperatures T_m and the molar enthalpy changes ΔH_{cal} under these conditions are summarized in Table 4.

This means that the chromatographically detected PQ9 molecules are partly located in the Q_A and Q_B sites and partly in the detergent shell or bound to PSIIcc in a different, functionally inactive position. Occupancy of approximately 30–45% of the Q_B binding sites in monomeric PSIIcc with plastoquinone PQ9 and 2–3 molecules PQ9 within the mixed protein/detergent

Table 5
Influence of 1 μM herbicides on the phase transition temperature T_m of dimeric PSIIcc measured with CD-spectroscopy at 220 nm

Herbicide	T_m (°C)
Without	71±0.5
Atrazin	75.4±0.5
DCMU	72.4±0.8
Ioxynil	71.8±0.8
Monomeric PSIIcc	67.6±0.7

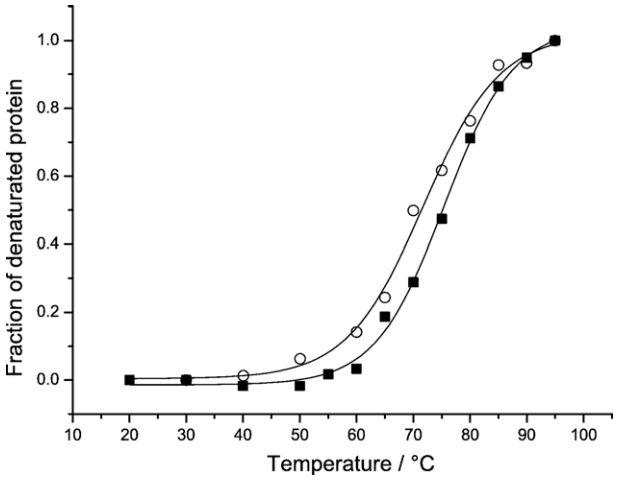

Fig. 6. Denaturation of dimeric PSIIcc induced by a temperature increase as observed with CD-spectroscopy. Fraction of unfolded dimeric PSIIcc measured at 220 nm between 20 and 90 °C in the absence (○) and presence of 1 μM atrazin (■).

micell may cause stoichiometries <1 for herbicide binding due to competitive effects. This could serve as explanation why strongly binding herbicides like terbutryn and atrazin exhibit higher stoichiometries compared to weaker binding bromoxynil and bromacil. To test this hypothesis, we measured the stoichiometries for bromacil binding after illumination of the PSIIcc probe in the presence of dithionite (data not shown). But even under this conditions where PQ9 should dissociate from the Q_B site, the low stoichiometries for bromacil are not enhanced.

Gleiter at al. [40] suggested that the Q_B binding sites are probably damaged with increasing amounts of detergent necessary for solubilization of PSIIcc particles. Since the Q_B-sites are formed by loops exposed to the solvent, it might be possible that during solubilization a close contact between β-DM and the Q_B binding site occurs. Therefore, dissociation constants for herbicides should be increased for detergent-solubilized PSIIcc compared with thylakoid membrane fragments from spinach. In contrast to these findings, Reifler et al. [36] demonstrated that binding constants for thylakoid membrane fragments and detergent-solubilized PSIIcc from *Thermosynechococcus* sp. are nearly identical. Their pI_{50} values for the inhibition of O_2 evolution of detergent-solubilized extracts from *Thermosynechococcus* sp. by herbicides like atrazin and DCMU [36] fall in the same range as reported in the literature for thylakoid fragments [35].

We cannot clarify if binding of herbicides to thylakoids is comparable with the binding to PSIIcc because binding constants for complexation of herbicides to thylakoid membrane fragments cannot be determined with the ITC technique. Analytical ultracentrifugation and dynamic light scattering showed that monomeric PSIIcc is only stable at 0.03 to 0.11 mg/ml, whereas at concentrations between 0.65 and 2 mg/ml higher aggregates with molar mass ≈1400 kDa are formed, indicating tri- or tetramers of PSIIcc [16]. At PSIIcc protein concentrations of 10 mg/ml used in the ITC experiments, these aggregates probably exist and it is possible that not all binding sites are accessible for weak herbicide binding due to the

formation of higher aggregates at the concentrations used for ITC while strongly binding herbicides such as terbutryn bind with stoichiometries close to 1. In general a fraction of monomeric and dimeric PSIIcc was resistant to inhibition of the oxygen-evolving activity even at very high inhibitor concentration.

Modification of the Q_B site is also supported by our flash fluorescence measurements. In case of the monomeric PSIIcc the time constant of the middle phase, which reflects the binding of PQ9 to the Q_B site following the flash was substantially slower than in the dimeric cores. In addition, the large slow phase of the decay shows that in about 60% of monomeric PSIIcc the $PQ9^-$ bound to the Q_A binding site recombines with the S_2 state of the water oxidizing complex in the absence of DCMU. This indicates that either the Q_A to Q_B electron transport is completely blocked in this fraction of monomeric centers, or that the redox potential of Q_B is shifted close to that of Q_A. This latter possibility is supported by the slowed down fast phase (3.7 ms) that indicates a decreased driving force for electron transfer between Q_A and Q_B. In dimeric PSIIcc, where the slow recombination phase arises only in 24% of the particles, Q_A^- can be repopulated largely via the $Q_A^-Q_B \leftrightarrow Q_AQ_B^-$ equilibrium indicating a (partly) functional Q_B site.

The flash fluorescence measurements performed in the presence of DCMU reveal an almost complete blockage of the Q_A to Q_B electron transfer. However, it is quite possible that the residual oxygen evolving activity is due to a competition between the artificial electron acceptor and the inhibitors at the partly modified Q_B site (this notion is supported by our flash fluorescence measurements in spinach BBY particles showing that DCBQ can accept electrons in the presence of high concentration of DCMU in about 20% of centers).

In contrast to exothermic binding reactions observed for herbicides in general, the binding of ioxynil and bromoxynil was endothermic with positive values for the binding enthalpy ΔH_b. Of all herbicides studied terbutryn forms the most stable complexes with monomeric PSIIcc as shown by ITC and DSC experiments. Terbutryn exhibits the largest value of the stoichiometry $n = 0.84$ (Table 1) and yielded the highest values of ΔH_b for binding (Table 2) and ΔH_{cal} (Table 4a) of the unfolding reaction probably due to the high stability of its complex with monomeric PSIIcc (Table 4a, Fig. 5a). In the case of monomeric PSIIcc the effect of herbicide binding on ΔH_{cal} seems to correlate with the values of ΔH_b measured by ITC: herbicides with endothermic binding processes (i.e. ioxynil and bromoxynil; Table 2) result in a decreased ΔH_{cal}, while herbicides with an exothermic binding reaction lead to increased values of ΔH_{cal}. Binding of herbicides to dimeric PSIIcc generally results in a decrease of ΔH_{cal}, with a maximum effect evoked by trietazin. Further studies are required to analyze the putative correlation between ΔH_{cal} and ΔH_b.

To clarify the contribution of the heat of neutralization to the overall enthalpy change, ΔH_b, due to proton uptake or release to the buffer we measured the binding reaction of terbutryn to monomeric PSIIcc in buffers with different ionization energy. We found a linear relationship between the apparent enthalpy change of the binding reaction of terbutryn and the ionization energy of the employed buffers [41]. The intercept of this graph and the slope correspond to the corrected enthalpy change $\Delta H'_b = -33.5 \pm 0.4$ kJ/mol and the number $N = 0.41 \pm 0.02$ of protons released by the binding reaction between terbutryn and monomeric PSIIcc, respectively.

In spite of the low stoichiometries of several herbicide/PSIIcc complexes, ioxynil and terbutryn form stable complexes well suited for co-crystallization experiments of these herbicides with PSIIcc dimer for X-ray diffraction studies as also demonstrated for terbutryn and the bacterial reaction centre [42]. Preliminary co-crystallization studies of dimeric PSIIcc with ioxynil and terbutryn resulted in crystals diffracting X-rays to a maximum resolution of 5.0 Å and 3.4 Å respectively. This difference in diffraction properties for ioxynil and terbutryn cocrystals is in line with the observed tendency of destabilization or stabilization of PSII by the two herbicides.

In an forthcoming publication we will study in greater detail the influence of β-DM on the thermodynamics of herbicide binding to PSIIcc to address the problem of low stoichiometries. Also we will continue our study of the contribution of protonation reactions to the overall enthalpy change of herbicide binding and to determine the corrected values of $\Delta H'_b$ for the various herbicides. Based on the here described findings we hope to obtain a structure of PSIIcc with herbicide bound to the Q_B site in the near future. This will in combination with the detailed thermodynamic data of herbicide binding allow for a deeper understanding of the interaction between PSIIcc and its inhibitors.

Note added in proof

The 3.0 Å resolution structure of PSII has been published recently [43].

Acknowledgements

This work was supported by DFG-Sonderforschungsbereich 498 and by a grant from the Hungarian Granting Agency, OTKA (T 34321). The authors would like to thank D. DiFiore and C. Lüneberg for technical assistance and Dr. S. Iskandrova for flash-induced fluorescence relaxation kinetic measurements.

References

[1] B. Ke, Photosynthesis-photobiochemistry and respiration, Advances in Photosynthesis and Respiration, vol. 10, Kluwer Academic Publishers, Dordrecht, The Netherlands, 2001.
[2] R.D. Britt, Oxygen evolution, in: D.R. Ort, C.F. Yocum (Eds.), Oxygenic Photosynthesis: The Light Reactions, Kluwer Academic Publishing, Dordrecht, The Netherlands, 1996, pp. 137–164.
[3] R.J. Debus, The manganese and calcium ions of photosynthetic oxygen evolution, Biochim. Biophys. Acta 1102 (1992) 269–352.
[4] C.W. Hoganson, G.T. Babcock, A metalloradical mechanism for the generation of oxygen from water in photosynthesis, Science 277 (1997) 1953–1956.
[5] J.H. Nugent, A.M. Rich, M.C. Evans, Photosynthetic water oxidation: towards a mechanism, Biochim. Biophys. Acta 1503 (2001) 138–146.
[6] J. Barber, Photosystem II: the engine of life, Q. Rev. Biophys. 36 (2003) 71–89.

[7] G. Renger, Photosynthetic water oxidation to molecular oxygen: apparatus and mechanism, Biochim. Biophys. Acta 1503 (2001) 210–228.
[8] B.A. Diner, G.T. Babcock, Structure, dynamics and energy conversion efficiency in photosystem II, in: D.R. Ort, C.F. Yocum (Eds.), Oxygenic Photosynthesis: The Light Reactions, Kluwer Academic Publishing, Dordrecht, The Netherlands, 1996, pp. 213–247.
[9] A.R. Crofts, C.A. Wraight, The electrochemical domain of photosynthesis, Biochim. Biophys. Acta 726 (1983) 149–185.
[10] W. Oettmeier, Herbicide resistance and supersensitivity in photosystem II, Cell Mol. Life Sci. 55 (1999) 1255–1277.
[11] A.W. Rutherford, A.R. Crofts, Y. Inoue, Thermoluminescence as probe of Photosystem II photochemistry. The origin of flash-induced glow peak, Biochim. Biophys. Acta 682 (1982) 457–465.
[12] A. Trebst, Inhibitors in electron flow: tools for the functional and structural localization of carriers and energy conservation sites, Methods Enzymol. 69 (1980) 675–715.
[13] G. Renger, Herbicide interaction with photosystem 2. Recent development, Physiol. Veg. 24 (1986) 509–521.
[14] N. Ginet, J. Lavergne, Equilibrium and kinetic parameters for the binding of inhibitors to the QB pocket in bacterial chromatophores: dependence on the state of QA, Biochemistry 40 (2001) 1812–1823.
[15] J. Kern, B. Loll, C. Lüneberg, D. DiFiore, J. Biesiadka, K.-D. Irrgang, A. Zouni, Purification, characterisation and crystallisation of photosystem II from *Thermosynechococcus elongatus*, Biochim. Biophys. Acta 1706 (2005) 147–157.
[16] A. Zouni, J. Kern, J. Frank, T. Hellweg, J. Behlke, W. Saenger, K.-D. Irrgang, Size determination of cyanobacterial and higher plant Photosystem II by gel permeation chromatography, light scattering and ultracentrifugation, Biochemistry 44 (2005) 4572–4581.
[17] K. Gounaris, D.J. Chapman, J. Barber, Isolation and characterisation of D1/D2/cytochrome b559 complex from Synechocystis 6803, Biochim. Biophys. Acta 973 (1989) 296–301.
[18] O. Nanba, K. Satoh, Isolation of a photosystem II reaction center consisting of D-1 and D-2 polypeptides and cytochrome b-559, Proc. Natl. Acad. Sci. U. S. A. 84 (1987).
[19] J. Biesiadka, B. Loll, J. Kern, K.-D. Irrgang, A. Zouni, Crystal structure of cyanobacterial photosystem II at 3.2 Å resolution: a closer look at the Mn-cluster, PCCP, Phys. Chem. Chem. Phys. 6 (2004) 4733–4736.
[20] A. Zouni, H.-T. Witt, J. Kern, P. Fromme, N. Krauß, W. Saenger, P. Orth, Crystal structure of photosystem II from *Synechococcus elongatus* at 3.8 A resolution, Nature 409 (2001) 739–743.
[21] J. Kern, B. Loll, A. Zouni, W. Saenger, K.-D. Irrgang, J. Biesiadka, Cyanobacterial photosystem II at 3.2 Å resolution—The plastochinone binding pockets, Photosynth. Res. 84 (2005) 153–159.
[22] G.H. Schatz, H.T. Witt, Extraction and characterisation of oxygen-evolving Photosystem II complexes from a thermophilic cyanobacterium Synechococcus spec, Photobiochem. Photobiophys. 7 (1984) 1–14.
[23] R.J. Porra, W.A. Thompson, P.E. Kriedemann, Determination of accurate extinction coefficients and simultaneous-equations for assaying chlorophyll a and chlorophyll b extracted with 4 different solvents—Verification of the concentration of chlorophyll standards by atomic absorption spectroscopy, Biochim. Biophys. Acta 975 (1989) 384–394.
[24] D.F. Ghanotakis, G.G. Tsiotis, T.M. Bricker, Polypetides of photosystem II, in: G.S. Singhal, G. Renger, S.K. Sopory, K.-D. Irrgang, Govindjee (Eds.), Concepts in Photobiology: Photosynthesis and Photomorphogenesis, Narosa Publishing House, New Dehli, India, 1999, pp. 264–291.
[25] B.A. Barry, R.J. Boerner, L.C.a.d. Paula, The use of cyanobacteria in the study of the structure and function of photosystem II, in: D.A. Bryant (Ed.), The Molecular Biology of Cyanobacteria, Kluwer Academic Publishers, Dordrecht, Netherlands, 1994, pp. 217–257.
[26] J.R. Livingstone, Antibody characterization by isothermal titration calorimetry, Nature 384 (1996) 491–492.
[27] T. Wiseman, S. Willistone, J.F. Brandts, L.-N. Lin, Rapid measurement of binding constants and heats of binding using a new titration calorimeter, Anal. Bioch. 179 (1989) 131–137.
[28] L.C. Clark, Monitor and control of blood and tissue oxygen tensions, Trans. Am. Soc. for Artifi. Int. Organs 2 (1956) 41.
[29] M. Trtilek, D.M. Kramer, M. Koblizek, Dual-modulation LED kinetic fluorometer, J. Lumin. 72–74 (1997) 597–599.
[30] I. Vass, D. Kirilovsky, A.-L. Etienne, UV-B radiation-induced donor- and acceptor-side modifications of Photosystem II in the cyanobacterium Synechocystis sp. PCC 6803, Biochemistry 38 (1999) 12786–12794.
[31] A. Joliot, P. Joliot, Etude cinétique de la réaction photochimique libérant l'oxygéne au cours de la photosynthése, C. R. Acad. Sci. 258 (1964) 4622–4625.
[32] C.N. Pace, Determination and analysis of urea and guanidine hydrochloride denaturation curves, Methods Enzymol. 131 (1986) 266–280.
[33] R.d. Wijn, H.J.V. Gorkom, Kinetics of electron transfer from QA to QB in photosystem, Biochemistry 40 (2001) 11912–11922.
[34] G. Renger, H.-J. Eckert, A. Bergmann, J. Bernarding, B. Liu, A. Napiwotzki, F. Reifarth, H.-J. Eichler, Fluorescence and spectroscopic studies of exciton trapping and electron transfer in Photosystem II of higher plants, Aust. J. Plant Physiol. 22 (1995) 167–181.
[35] C. Fedtke, Biochemistry and Physiology of Herbicide Action, Springer Verlag, New York, NY, 1982.
[36] M.J. Reifler, V.A. Sazalai, C.N. Peterson, G.W. Brudvig, Effects of tail-like substituents on the binding of competitive inhibitors to the QB site of photosystem II, J. Mol. Recognit. 14 (2001) 157–165.
[37] T. Ohno, K. Satoh, S. Katoh, Chemical composition of purified oxygen-evolving complexes from the thermophilic cyanobacterium Synechococcus sp. Biochim. Biophys. Acta 852 (1986) 1–8.
[38] X.-S. Tang, B.A. Diner, Biochemical and spectroscopic characterization of a new oxygen-evolving photosystem II core complex from the Cyanobacterium Synechocystis PCC 6803, Biochemistry 33 (1994) 4594–4603.
[39] A. Zouni, J. Kern, B. Loll, P. Fromme, H.T. Witt, P. Orth, N. Krauss, W. Saenger, J. Biesiadka, Biochemical characterization and crystal structure of water oxidizing photosystem II from *Synechococcus elongatus*, 12th International Congress on Photosynthesis, CSIRO Publishers, 2001, pp. S05–S003.
[40] H.G. Gleiter, E. Haag, Y. Inoue, G. Renger, Functional characterisation of a purified homogeneous Photosystem II core complex with high oxygen evolution capacity from spinach, Photosynth. Res. 35 (1993) 41–53.
[41] I. Jelesarov, H.R. Bosshard, Thermodynamics of ferredoxin binding to ferredoxin:NADP+ reductase and the role of water at the complex interface, Biochemistry 33 (1994) 13321–13328.
[42] C.R. Lancaster, M.V. Bibikova, P. Sabatino, D. Oesterhelt, H. Michel, Structural basis of the drastically increased initial electron transfer rate in the reaction center from a *Rhodopseudomonas viridis* mutant described at 2.00–A resolution, J. Biol. Chem. 275 (2000) 39364–39368.
[43] B. Loll, J. Kern, W. Saenger, A. Zouni, J. Biesiadka, Towards complete cofactor arrangement in the 3.0 Angstrom resolution structure of photosystem II, Nature 438 (2005) 1040–1044.